

Enrichment and description of novel bacteria performing syntrophic propionate oxidation at high ammonia level

Abhijeet Singh , Anna Schnürer and Maria Westerholm *

Department of Molecular Sciences, Swedish University of Agricultural Sciences, Uppsala, SE-750 07, Sweden.

Summary

Inefficient syntrophic propionate degradation causes severe operating disturbances and reduces biogas productivity in many high-ammonia anaerobic digesters, but propionate-degrading microorganisms in these systems remain unknown. Here, we identified candidate ammonia-tolerant syntrophic propionate-oxidising bacteria using propionate enrichment at high ammonia levels ($0.7\text{--}0.8\text{ g NH}_3\text{ L}^{-1}$) in continuously-fed reactors. We reconstructed 30 high-quality metagenome-assembled genomes (MAGs) from the propionate-fed reactors, which revealed two novel species from the families Peptococcaceae and Desulfobulbaceae as syntrophic propionate-oxidising candidates. Both MAGs possess genomic potential for the propionate oxidation and electron transfer required for syntrophic energy conservation and, similar to ammonia-tolerant acetate degrading syntrophs, both MAGs contain genes predicted to link to ammonia and pH tolerance. Based on relative abundance, a Peptococcaceae sp. appeared to be the main propionate degrader and has been given the provisional name “*Candidatus Syntrophopropionicum ammoniitolerans*”. This bacterium was also found in high-ammonia biogas digesters, using quantitative PCR. Acetate was degraded by syntrophic acetate-oxidising bacteria and the hydrogenotrophic methanogenic community consisted of *Methanococcus bourgensis* and a yet to be characterised *Methanoculleus* sp. This work provides knowledge of cooperating syntrophic species in high-ammonia systems and reveals that ammonia-tolerant syntrophic propionate-degrading populations share common

features, but diverge genomically and taxonomically from known species.

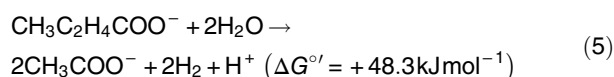
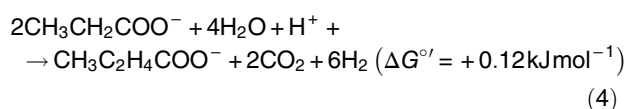
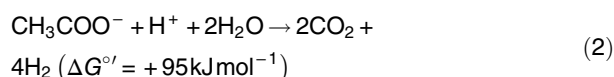
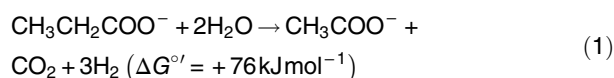
Introduction

Syntrophic interactions are essential for complete degradation of organic compounds in a variety of natural anaerobic environments and in engineered bioreactors for biogas production (McInerney *et al.*, 2009). Interactions of particular importance involve bacteria and methanogens performing syntrophic degradation of short-chain fatty acids (e.g., acetate, propionate), since these acids rapidly acidify the environment if not consumed. Accumulation of propionate is undesirable, since it results in process instability and a significant decline in methane production (Ahring, 2003; Chen *et al.*, 2014). Due to thermodynamic restrictions, fatty acid degradation requires acetate-cleaving methanogenesis and/or syntrophic oxidising interactions that involve two or more microorganisms. The oxidation of short-chain fatty acids is endergonic under standard conditions, but as the end-products from the first bacterial consumer are instantly degraded by cooperating methanogens the overall reaction become exergonic (Dolfing, 2014). Nevertheless, these reactions allow microorganisms to survive on minimal energy resources, which inevitably leads to slow acid degradation rates (Morris *et al.*, 2013). Fatty acid accumulation is a persistent challenge in anaerobic degradation of protein-rich materials, due to the generally high content of toxic ammonia in these processes (Capson-Tojo *et al.*, 2020). Ammonia is toxic to microorganisms and in particular methanogens that convert acetate to methane. The restricted methanogenic activity results in increased levels of acetate and hydrogen, which in turn affects the degradation of other fatty acids, such as propionate. Extensive work has been conducted to identify operational strategies that can abate acetate accumulation and improve biogas production in high-ammonia biogas processes (Westerholm *et al.*, 2016). However, propionate degradation at high ammonia levels has been less extensively studied. Understanding microbial relationships that drive propionate degradation would assist

Received 27 May, 2020; revised 15 September, 2020; accepted 2 January, 2021. *For correspondence. E-mail maria.westerholm@slu.se; Tel. (+46) 18 67 10 00; Fax (+46) 18 67 20 00

in development of effective management strategies for high-ammonia anaerobic degradation systems.

In anaerobic systems with limited levels of sulphate, propionate is degraded through either a syntrophic or a dismutation pathway. In the syntrophic pathway, propionate is converted to acetate, bicarbonate and H₂ or formate (Eq. 1) by syntrophic propionate-oxidising bacteria (SPOB) (Schink, 1997; Hidalgo-Ahumada *et al.*, 2018; Chen *et al.*, 2020).



Removal of H₂ and/or formate by methanogens is essential for SPOB activity (Eq. 3), due to thermodynamic constraints. Depletion of acetate (Eq. 2) has also been shown to increase the rate of propionate degradation (de Bok *et al.*, 2004). In the dismutating pathway, propionate is converted to acetate and butyrate, i.e. oxidised and reduced compounds are formed simultaneously (Eq. 4), after which butyrate is oxidised to acetate (Eq. 5) (Liu *et al.*, 1999; de Bok *et al.*, 2001). The SPOB isolated to date belong to the genera *Syntrophobacter* (Boone and Bryant, 1980), *Syntrophobacterium* (Wallrabenstein *et al.*, 1995; Harmsen *et al.*, 1998; Chen *et al.*, 2005; 2021), *Smithella* (Liu *et al.*, 1999), *Pelotomaculum* (Imachi *et al.*, 2002; de Bok *et al.*, 2005; Imachi *et al.*, 2007) and *Desulfotomaculum* (formerly *Desulfotomaculum*) (Plugge *et al.*, 2002; Bertran *et al.*, 2020). Other SPOB candidates are suggested to belong to the genera *Cryptanaerobacter*, *Desulfotomaculum*, *Smithella*, *Syntrophomonas*, *Syntrophobacter*, *Pelotomaculum*, “*Candidatus Cloacamonas*” and “*Candidatus Syntrophosphaera*” (Shigematsu *et al.*, 2006; Ariesyady *et al.*, 2007a; Pelletier *et al.*, 2008; Ahlert *et al.*, 2016; Maus *et al.*, 2016b; Li *et al.*, 2018; Dyksma and Gallert, 2019; Zheng *et al.*, 2019; Chen *et al.*, 2020). Biochemical, genomics and transcriptomics studies have provided insights into use of the methylmalonyl-CoA pathway for propionate oxidation by all known SPOB with the exception of *Smithella*, which converts propionate through the dismutating pathway (Harmsen *et al.*, 1998; de Bok *et al.*, 2001; Imachi

et al., 2002; Hidalgo-Ahumada *et al.*, 2018). However, all characterised and putative SPOB identified to date, and information on their metabolic function, derive from studies in low-ammonia environments and these SPOB have not been observed in high-ammonia processes (Westerholm *et al.*, 2015; Bonk *et al.*, 2018). Despite syntrophic microorganisms playing an essential role in the anaerobic degradation process, they grow slowly and generally constitute a minor part of the total microbial community in anaerobic digesters. This often obstructs detection of syntrophic populations in systems containing microbial communities degrading mixed substrates (Vanwonterghem *et al.*, 2014; Kirkegaard *et al.*, 2017). Consequently, there is a need to reveal identities and gain a fundamental understanding of the requirements for growth and activity of ammonia-tolerant SPOB, which can help in steering the biogas process to circumvent accumulation of propionate.

In this study, we enriched propionate-degrading communities from high-ammonia anaerobic systems in continuously-fed reactors and looked for putative ammonia-tolerant SPOB. 16S rRNA gene amplicon sequencing was used to determine discrepancies in microbial community structure between two acetate- and two propionate-fed reactors, while metagenomic sequencing was used to reveal the genetic repertoire of the SPOB candidates identified. The study provides insights into the ecology and metabolic function of ammonia-tolerant syntrophic propionate-oxidising bacteria originating from biogas-producing digester systems.

Results and Discussion

Anaerobic reactor performance

All four propionate-fed (P1, P2) and acetate-fed reactors (A1, A2) used in the present study were operated at mesophilic (37°C) conditions for 144 days (115 days for P2) and were inoculated with sludge from a high-ammonia biogas digester. The continuously acetate-fed reactors had average daily gas production of 0.03–0.05 L day⁻¹, with 47%–53% methane content (days 24–129). The continuously propionate-fed reactors initially had average daily methane production of 0.02 L day⁻¹ (days 24–80), which then increased to 0.1 L day⁻¹ (days 80–115/144). The average methane content was 56%–59% in P1 and P2 over the course of the study (Fig. 1, Table S1). The pH in the continuously-fed reactors varied between 7.9–8.1, providing an ammonia-nitrogen level of 0.4–0.6 g NH₃-N L⁻¹. This ammonia level inhibits many microorganisms and thus commonly causes a reduction in methane production rates and accumulation of short-chain fatty acids, even in ammonia-adapted biogas processes (Capson-Tojo *et al.*, 2020).

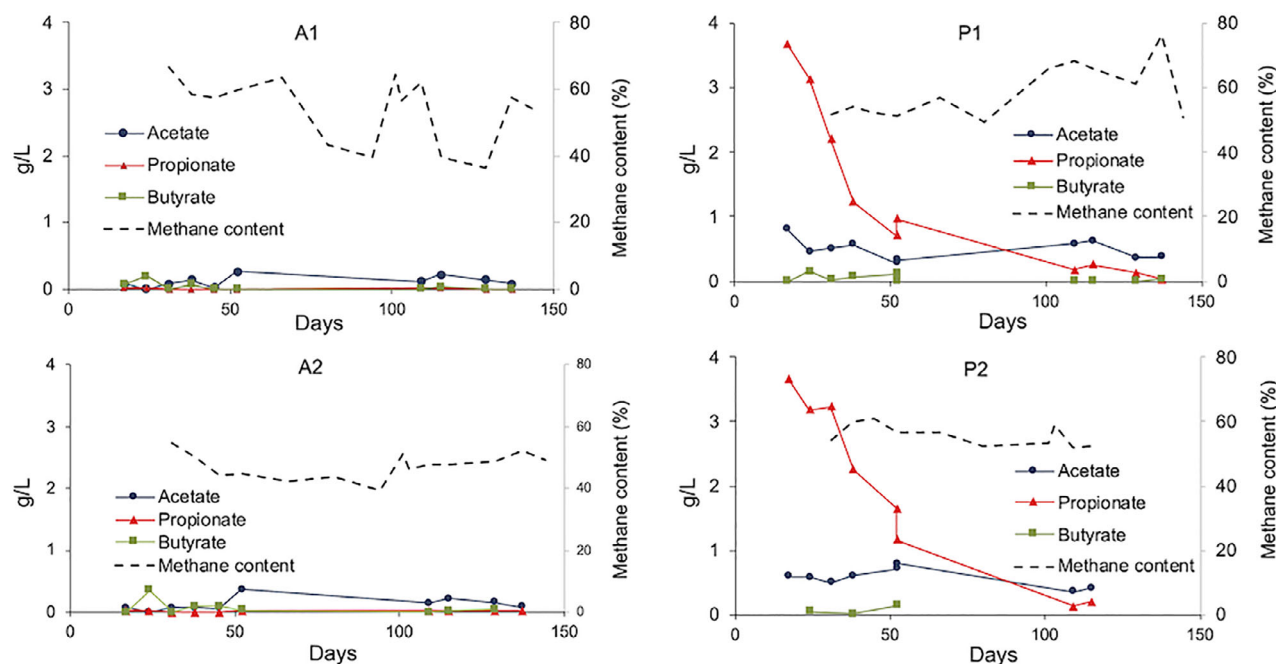


Fig 1. Propionate, acetate and butyrate concentrations and methane content in the produced gas in replicate reactors continuously fed acetate (A1, A2) or propionate (P1, P2). Due to technical error P2 had to be shut-down after 115 days of operation. [Color figure can be viewed at wileyonlinelibrary.com]

Within the first 20 days of operation of the two acetate-fed reactors, the syntrophic acetate-degrading community had reduced acetate levels from the initial concentration of 8.9 g L^{-1} to $< 0.4 \text{ g L}^{-1}$ (Fig. 1). This is in agreement with findings in previous studies on acetate-fed reactors under similar operating conditions (Westerholm *et al.*, 2018b). The propionate-degrading community had a longer lag phase for growth, and propionate levels in the effluent from the propionate-fed reactors (P1 and P2) decreased from 4 g L^{-1} within the first 20 days to reach levels below 0.5 g L^{-1} after about 100 days of operation. The decrease in propionate level coincided with the increased gas production during this period. The concentration of acetate in the propionate-fed reactors remained relatively constant at around 0.5 g L^{-1} over the course of the study (Fig. 1, Table S1), indicating that product inhibition by acetate was likely not the reason for the observed relatively slow decrease in propionate levels. The other short-chain fatty acids analysed (butyrate, isobutyrate, valerate, isovalerate, capronate and isocaproate) were not detected in any of the continuously fed reactors.

Microbial community structure in the acetate- and propionate-fed reactors

The 16S rRNA gene amplicon sequencing demonstrated abundance of as yet unclassified taxa assigned as ST-12K33 (48%–67%, class Sphingobacteriia, phylum

Bacteroidetes), Thermoanaerobacterae (7%–30%) and Clostridaceae_2 (3%–47%, Clostridia, Firmicutes) in all four continuously-fed reactors during the initial operating period (day 17) (Fig. 2, Figs. S1 and S2). Thermoanaerobacterae remained at a similar level, but the ratio of ST-12K33 and Clostridaceae_2 decreased over the course of the study ($< 32\%$) in all reactors. Instead, the family Pseudomonadaceae (Gammaproteobacteria, Proteobacteria) increased from below detection to 10%–67% (Fig. 2). Comparing the reactors revealed lower levels of Clostridaceae_2 and Pseudomonadaceae and higher abundance of ST-12K33 in the propionate-fed than in the acetate-fed reactors (days 31–115) (Fig 2).

The four acetate- and propionate-fed reactors had high relative abundance (3%–32%) of putative syntrophic acetate-oxidising bacteria affiliated with the family Clostridiaceae previously identified by Westerholm *et al.* (2018b) (in that previous study assigned as M_HC, 16S rRNA gene GenBank accession number MG35 6789). A metagenome-assembled genome retrieved in the present study (MAG 64) also affiliated with this species (Table S2).

Further comparison of the profiles developed over time in the reactors on family level revealed higher relative abundance of the family Peptococcaceae (class Clostridia) in the two propionate-fed reactors than in the acetate-fed reactors (days 30–115) (Fig. 2). Moreover, in one of the propionate-fed reactors the families

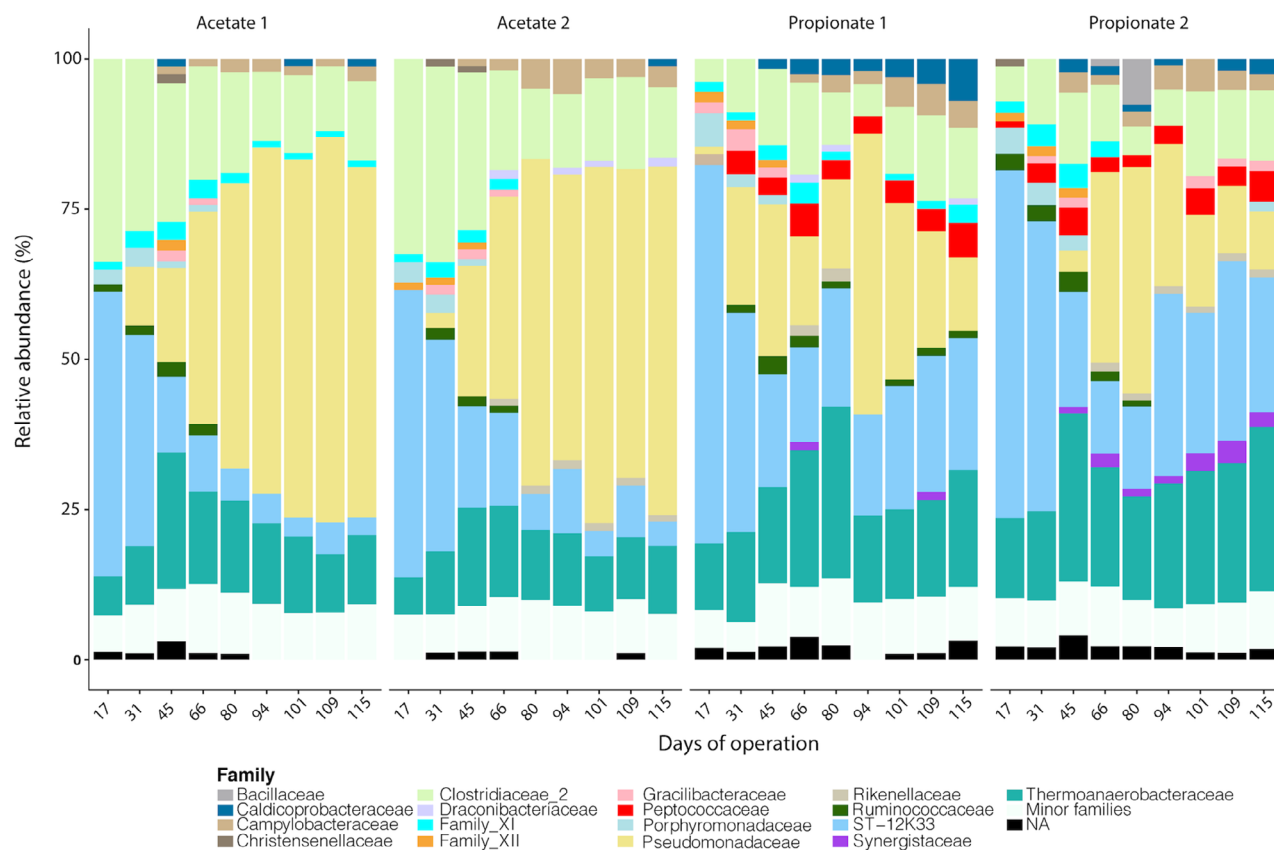


Fig 2. Microbial community structure on family level determined by 16S rRNA gene sequencing in acetate-fed and propionate-fed chemostats over the course of the study. Families representing < 1% (including archaeal sequences) are grouped into the black bar section designated “Minor families.” “*Candidatus Syntrophopropionicum ammoniitolerans*” (MAG 62) belongs to the family Peptococcaceae (red section if figure). [Color figure can be viewed at wileyonlinelibrary.com]

Caldicoprobacteraceae and Ruminococcaceae (Clostridia, chemostat P1) or the family Synergistaceae (class Synergistia, phylum Synergistetes, chemostat P2) explicitly increased in comparison with the acetate-fed reactors (days 45–115) (Fig. 2). Archaeal sequences were found to represent < 0.3% in the 16S rRNA gene amplicon sequencing approach in all samples and were foremost affiliated to the genus *Methanoculleus* (class Methanomicrobia).

Metagenome sequencing of samples taken from the propionate-fed reactors (day 115) and individual metagenome assembly and genome binning resulted in reconstruction of 29 metagenome-assembled genomes (MAGs) with genome completeness above 70% and contamination below 4% (with the exception of the two Euryarchaeota MAGs that had 5%–10% contamination). Twenty-five of the constructed genomes belonged to previously unknown and little studied bacterial taxa (< 60% average genomic amino acid identity to closest relative) (Table S2). Most MAGs affiliated with the phylum Firmicutes and with the orders Thermoanaerobacterales ($n = 5$), Clostridiales (5) and Bacillales (4). The remaining

MAGs were positioned in the phyla Bacteroidetes (3), Chloroflexi (1), Euryarchaeota (1), Proteobacteria (2), Spirochaetes (4), Synergistetes (1) and Tenericutes (1). The coverage of MAGs obtained in metagenome sequencing revealed a community structure resembling the 16S rRNA gene sequencing profile, with high abundance of Sphingobacteriaceae 22%, Pseudomonadaceae (4%), Clostridiaceae (4%) and Thermoanaerobacteraceae (3%) (Fig. S3), with the exception that MAG 55 represented 15% of total recovered sequences in the metagenome sequencing. The inability of the primers used in the Illumina 16S rRNA gene sequencing to amplify the 16S rRNA gene of MAG 55 (Figs. S1 and S3) may have been due to methodological problems, for example, gaps in amplicon-based detection, which is a well-known problem (Morales and Holben, 2009; Eloë-Fadrosch *et al.*, 2016). Genome-to-genome distance calculations indicated that MAG 55 belonged to a phylum not represented in public databases ($\rho = 0.33$). Genes currently known to be required for propionate oxidation were absent in MAG 55, so this genome was not considered further in the present study.

Two Euryarchaeota genome assemblies (MAG 28, MAG 54) affiliating with the genus *Methanoculleus* were retrieved from the propionate-fed reactors (Table S2). MAG 54 shared 98% average nucleotide identity with *M. bourgensis* MAB1, while MAG 28 was only assigned to genus level. Based on coverage estimates, the two *Methanoculleus* MAGs together represented 13%, whereas less than 1% of the 16S rRNA genes in the amplicon sequencing affiliated with Euryarchaeota, indicating underestimation of this group in the latter approach.

Identification of putative ammonia-tolerant SPOB

With the aim of identifying potential SPOB, we looked for genera that increased in relative abundance in the propionate-fed reactors, but not in the acetate-fed reactors, over the course of the experiment. Detailed analysis of genomic-specific metabolic potential, determined by profiling all the genes against databases (UniProt v. 2020_01, KEGG, HydDB, RefSeq), was also performed on all MAGs retrieved, to identify candidates. Based on the genomic content combined with the 16S rRNA gene results, the results revealed two MAGs (MAG 62 and MAG 45) with the potential to syntrophically oxidise propionate.

“*Candidatus Syntrophopropionicum ammoniitolerans*” (MAG 62)

Based on 16S rRNA gene sequencing and the genetic repertoire of the corresponding MAG 62, the most likely SPOB candidate in the propionate-fed reactors belonged to the family Peptococcaceae (phylum Firmicutes, class Clostridia, order Clostridiales). This Peptococcaceae species was below the detection limit in the acetate-fed reactors, but represented > 1% of the total community at day 17 in both propionate-fed reactors, and thereafter ranged between 2% and 6% of the total community in those reactors (Fig. 2). The family Peptococcaceae includes several known mesophilic and thermophilic SPOB (Imachi *et al.*, 2002; de Bok *et al.*, 2005; Imachi *et al.*, 2007).

MAG 62 had a completeness of 96% and constituted 2% of the total metagenome coverage (Table 1, Fig. S3). In phylogenetic assessment based on whole-genome sequencing, MAG 62 clustered with *Pelotomaculum propionicum*, while in assessment based on 16S rRNA gene retrieval from genome sequencing, MAG 62 clustered with members of the genera *Pelotomaculum* and *Cryptanaerobacter* (Fig. 3A and B), with 93%–94% nucleotide identity to *P. propionicum* and *Cryptanaerobacter phenolicus*.

Comparison of MAG 62 with available genomes of known species in the genera *Pelotomaculum*,

Desulfofundulus and “*Ca. Propionivorax syntrophicum F70*” revealed genome-to-genome distance values of 18%–21% and average nucleotide identity values of 66%–72% (Fig. S4). These are sufficiently low levels for delineating new species (recommended cut-off points are 70% DNA-DNA hybridisation value and 95% average nucleotide identity) (Goris *et al.*, 2007; Jain *et al.*, 2018). Moreover, the genomic distance of MAG 62 from other members of the Peptococcaceae family indicates that this bacterium will form a novel genus when isolated and characterised. As MAG 62 was the most likely SPOB candidate in the high ammonia propionate-fed reactors studied and was shown to be present in high-ammonia biogas digesters (Table S3), it has been given the provisional name “*Ca. Syntrophopropionicum ammoniitolerans*”.

Methylmalonyl-CoA pathway

MAG 62 encodes the conventional methylmalonyl-CoA pathway, including propionate activation and downstream hydrolysis of acetyl-CoA (*pct* gene, steps 1 and 11 in Fig. 4A), carboxylation to methylmalonyl-CoA (step 2), followed by isomerisation and formation of succinyl-CoA (steps 3 and 4), and the ATP-requiring conversion of succinyl-CoA to succinate (step 5). For the subsequent part of the pathway, genes encoding fumarate reductase (*frd*, step 6), enabling the energetically unfavourable oxidation of succinate to fumarate with methylmenaquinol as electron acceptor, were detected. Genes encoding enzymes that convert fumarate to malate (*fum*, step 7) and malate dehydrogenase (*mdh*, step 8), which catalyses the subsequent conversion of malate to oxaloacetate using NAD⁺ as electron acceptor, were also found. For conversion of pyruvate to acetyl-CoA, genes encoding ferredoxin-dependent oxidoreductases (*por/kor*, step 10) were annotated (Fig. 4A, Table S4).

The enzyme propionate CoA transferase encoded by the *pct* gene has been proposed to couple the first (propionate activation, energy-requiring) and the last (hydrolysis of acetyl-CoA, energy-generating) steps in propionate oxidation by *Pelotomaculum thermopropionicum* (Kato *et al.*, 2009; Liu and Lu, 2018). The MAG 62 *pct* gene had 74% identity to the *pct* gene of *P. thermopropionicum* SI at nucleotide level. Genes for the AMP-dependent acyl-CoA synthetase (*asc*), proposed to catalyse the last acetate-forming step in *P. thermopropionicum* (Liu and Lu, 2018), were also found in MAG 62 (Fig. 4, Table S4). This enzyme is suggested to be involved in substrate activation in syntrophic degradation of other fatty acids, such as butyrate, benzoate and crotonate (James *et al.*, 2016; Hao *et al.*, 2020). Putative propionate transporter was not annotated in MAG 62 and the mechanisms for active or passive transport of propionate across the cell membrane of ammonia-tolerant SPOB remain to be determined. Genes

Table 1. General genome properties of the identified putative ammonia-tolerant syntrophic propionate-oxidising “*Ca. Syntrophopropionicum ammoniitolerans*” (MAG 62), *Desulfobulbaceae* sp. MAG 45 and the novel *Methanoculleus* sp. MAG 28 and MAG 54

	MAG 62	MAG 45	MAG 54	MAG 28
Length (bp)	2 363 537	2 457 827	2 323 366	2 042 409
Completeness (%)	96	93	81	82
Contamination (%)	2.7	2.7	3.8	5.2
GC content (%)	47.1	54.3	61.9	58.6
Total coding sequences (CDS)	2288	2224	2306	2064
Number of contigs	87	185	319	218
Total messenger RNA (mRNA)	2393	2291	2348	2100
Total transfer RNA (tRNA)	47	44	38	34

for oxaloacetate decarboxylase, an enzyme that has been proposed to couple conversion of oxaloacetate to pyruvate with extrusion of two sodium ions in “*Ca. Propionivorax syntrophicum*” (Hao *et al.*, 2020), were annotated in MAG 62 (step 9 in Fig. 4).

H₂/formate production and energy conservation systems

In syntrophic propionate oxidation, hydrogenases or formate dehydrogenases catalyse electron transfer from NADH or Fd_{red} (generated from substrate oxidation) to the final electron acceptors H⁺ and CO₂ (Stams and Plugge, 2009; Sieber *et al.*, 2012). In MAG 62, genes encoding [FeFe]-hydrogenases (group A) (Table S5), with similarities to hydrogenases present in *P. thermopropionicum* (Kosaka *et al.*, 2008), were found. This group comprises hydrogenases that bifurcate electrons between NAD, Fd and H₂, but can also be linked to formate dehydrogenase (Søndergaard *et al.*, 2016). In MAG 62, formate dehydrogenase units (including *fdhDE*, *iscS*) with associated molybdenum co-factors were annotated (Fig. 4A, Table S4). For some *Pelotomaculum* spp., formate dehydrogenases have been shown to be upregulated in co-culture compared with pure culture (Kato *et al.*, 2009; Hidalgo-Ahumada *et al.*, 2018; Liu and Lu, 2018). However, determination of the preferred electron carrier during propionate degradation by *Ca. S. ammoniacum* requires further investigation.

MAG 62 harbours genes coding proteins for flavin-based electron bifurcation that couples reduction of high- (e.g., NAD) and low-potential electron acceptors (e.g., ferredoxin) (Buckel and Thauer, 2018), including electron transfer flavoprotein (*etfAB*), heterodisulfide reductase (*hdrABC*) sulfhydrogenase beta subunit (*hydB*) and NAD(P) dehydrogenase. *Hdr* complexes have been hypothesised to play a role in sulphur metabolism, but have also been shown to be upregulated in association with propionate addition in culture of putative SPOB “*Ca. P. syntrophicum*” (Hao *et al.*, 2020). Ability of other SPOB to use electron bifurcation has been proposed, but using oxidoreductases (encoded by *rnf*, *nfn*) (Hidalgo-

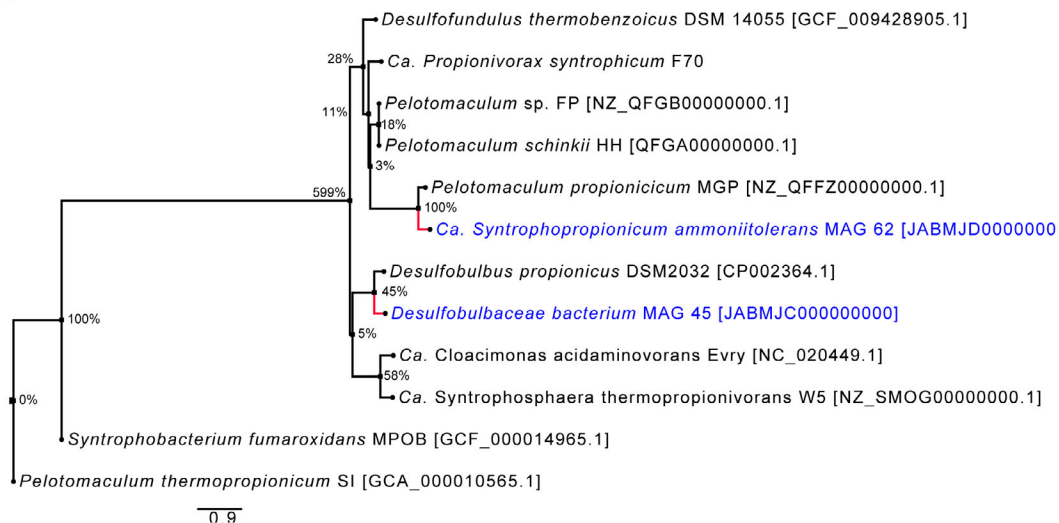
Ahumada *et al.*, 2018; Hao *et al.*, 2020), which were not found in MAG 62. No genes for cytochromes that support their function during respiration were annotated in MAG 62, but the MAG has genes encoding a complete ATP synthase complex that can be used for ATP formation (Fig. 4A, Table S4).

Potential energy conservation systems using ion-translocating pyrophosphatase have been presented for ammonia-tolerant syntrophic acetate-oxidising bacteria (Manzoor *et al.*, 2018) and for the putative SPOB (Pelletier *et al.*, 2008; Hao *et al.*, 2020). The genomic content of MAG 62 displayed genomic potential to use a similar mechanism. Pyrophosphatase (*hpp*, *ppa*) hydrolyses pyrophosphate (PP_i) and mediates the transport of cations (Na⁺/H⁺) against the electrochemical potential gradient, generating an ion motive force that can be used to produce ATP (Baykov *et al.*, 2013). MAG 62 also contains genes for water-soluble divalent electron quinone oxidoreductase (*wrbA*), which transfers electrons from the electron carrier NADH to quinone and is proposed to play a role in oxidative stress resistance (Green *et al.*, 2014). Moreover, MAG 62 encodes an oxalate/formate transporter (Fig. 4, Table S4), which might be used to accumulate formate inside the cell and then couple the transport of formate across the membrane with conservation of energy in the form of proton motive force, as previously suggested in SPOB (Hidalgo-Ahumada *et al.*, 2018).

Other metabolic capabilities, sporulation and motility

Key genes for the Wood-Ljungdahl pathway and the Calvin-Benson-Bassham cycle were absent in MAG 62, indicating inability for autotrophic carbon fixation (Cotton *et al.*, 2018). Complete sets of genes for glycolysis (glucose => pyruvate), gluconeogenesis (oxaloacetate => fructose-6P) and citrate cycle (second carbon oxidation, 2-oxoglutarate => oxaloacetate) were found, which indicates ability for heterotrophic growth on sugars in addition to propionate oxidation. For anabolic activities, genes for biosynthesis of amino acids, NAD,

A



B

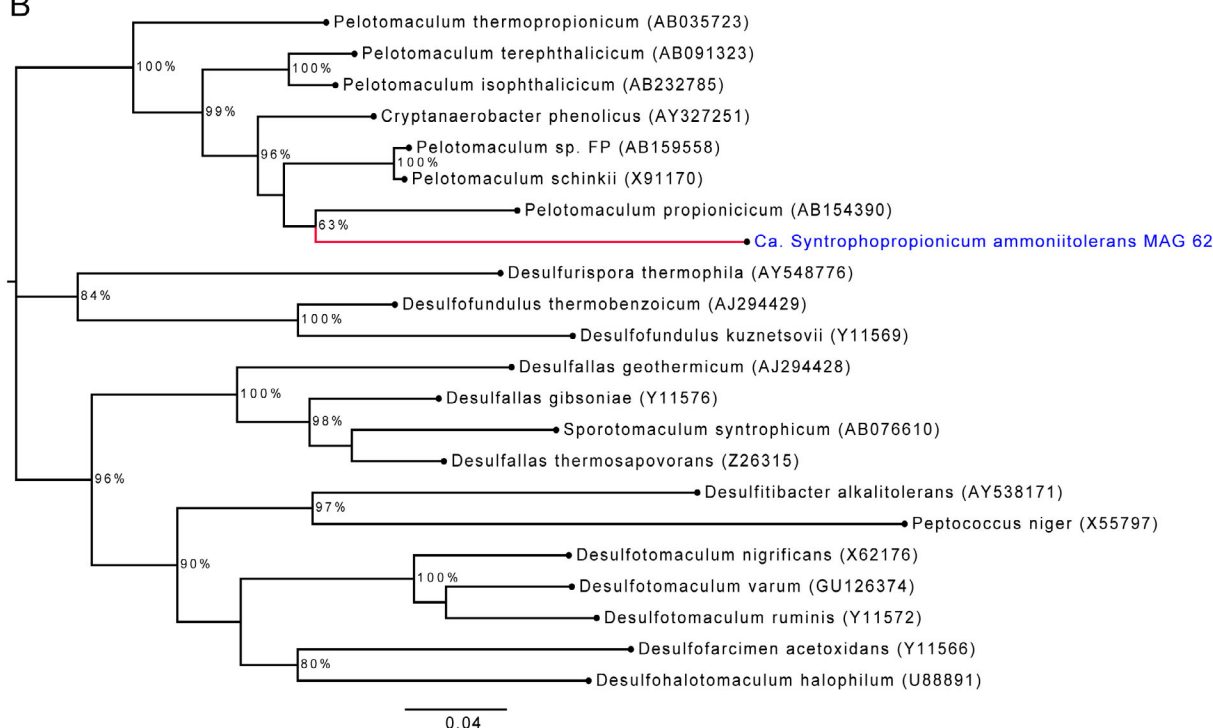


Fig 3. Phylogenetic relationships of “*Candidatus Syntrophopropionicum ammoniitolerans*” (MAG 62) with (A) known or putative syntrophic propionate-oxidising bacteria based on the whole-genome sequence and (B) closely related species of the family Peptococcaceae based on 16S rRNA gene sequences. Bootstrap values above 50% (per 1000 iterations) are shown at branch nodes. The whole-genome phylogenetic tree also includes *Desulfohalobaceae* sp. MAG 45 and values at branch nodes represent Species Tree inference from All Genes (STAG). Accession numbers for sequences used in the trees are given in brackets. [Color figure can be viewed at wileyonlinelibrary.com]

coenzyme and genes for the non-oxidative phase of the pentose phosphate pathway were annotated (Table S4). MAG 62 also contains genes encoding the complete flagellum biosynthesis machinery and a *motAB* encoding a complex that constitutes the transmembrane H⁺ channel, exerting force on the flagellar rotor (Nakamura and Minamino, 2019). Previous studies have indicated that

flagella play an important role in connecting *Pelotomaculum* with its partner methanogens (Ishii *et al.*, 2005; Hidalgo-Ahumada *et al.*, 2018; Liu and Lu, 2018). Gene annotation of catalases and superoxide dismutase [Mn/Fe] indicated some resistance to oxidative stress, while a broad set of genes previously shown to be involved in sporulation was also annotated (Table S4).

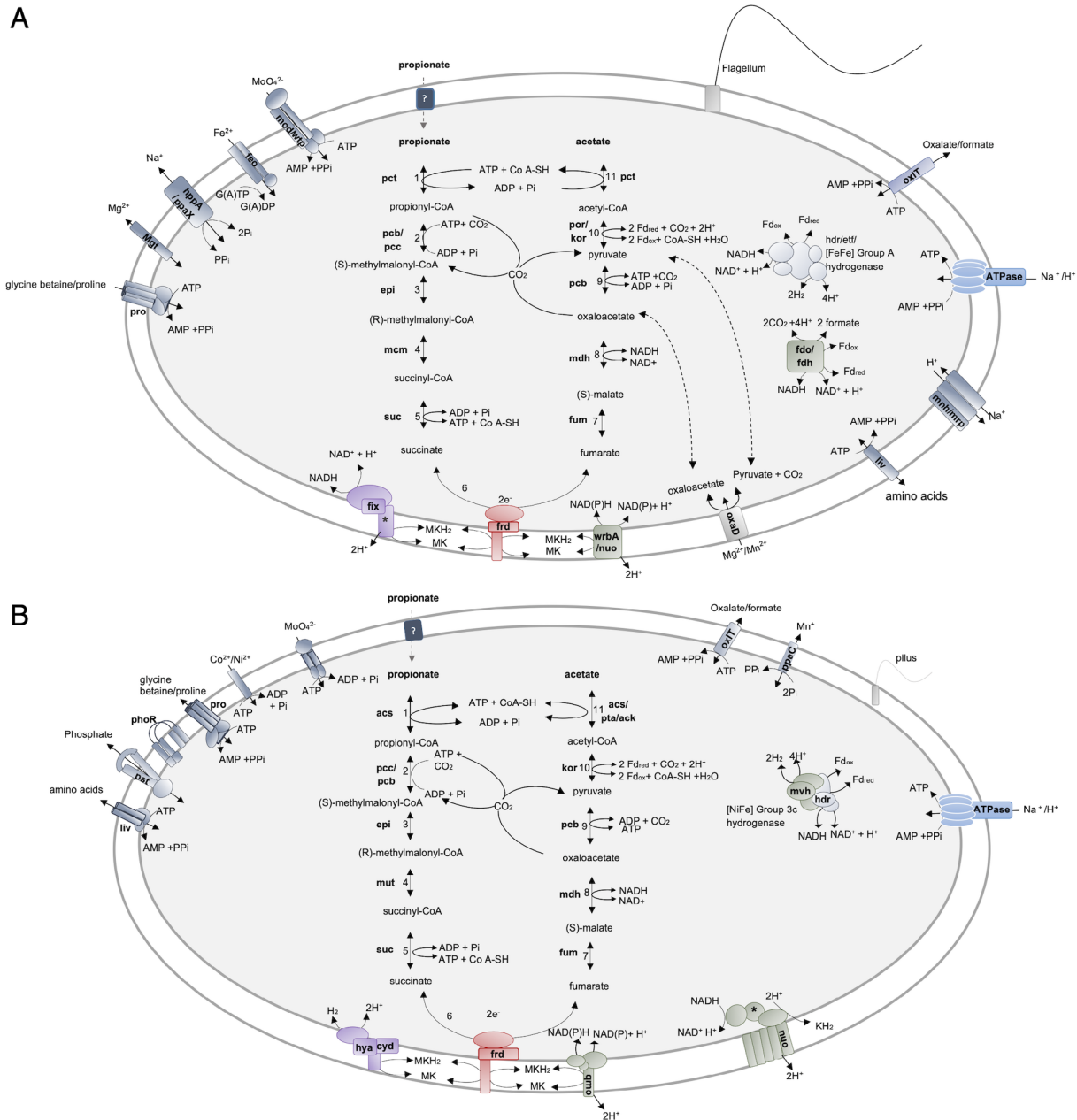


Fig 4. Genomic potential for propionate oxidation and electron transfer strategies required for syntrophic energy conservation in the proposed syntrophic propionate-oxidising bacteria. (A) “*Candidatus Syntrophopropionicum ammoniitolerans*” (MAG 62) and (B) *Desulfobulbaceae* MAG 45. Units marked with * were not found in the metagenome assembled genomes (MAGs). Genes encoding enzymes involved in methylmalonyl-CoA pathway include: *pct*—propionate CoA transferase, *pcc*—propionyl-CoA carboxylase, *epl*—methylmalonyl-Co epimerase, *mcm/mut*—methylmalonyl-Co mutase, *suc*—succinyl-CoA synthetase, *frd*—fumarate reductase, *fum*—fumarate hydratase, *mdh*—malate dehydrogenase, *por*—pyruvate ferredoxin oxidoreductase, *kor*—2-oxoglutarate/2-oxoacid ferredoxin oxidoreductase. [Color figure can be viewed at wileyonlinelibrary.com]

Abundance of “*Ca. Syntrophopropionicum ammoniitolerans*” (MAG 62) in the continuously fed reactors and in high-ammonia biogas digesters, and impact of NaCl

In the acetate-fed reactors, MAG 62 16S rRNA gene abundance was detected at a level of 3.9–4.1 log gene

copies ng^{-1} DNA at day 17, but the abundance was thereafter below detection limit (10^2 gene copies ng^{-1} DNA). MAG 62 abundance in the propionate-fed reactors was 3.9–4.7 log gene copies ng^{-1} DNA throughout the experimental period. The stable levels of MAG 62 indicate that this bacterium was not washed out, suggesting a

shorter doubling time than the retention time of the continuously fed reactors (28 days) under the conditions prevailing in this study. This is consistent with doubling times reported from known SPOB in co-culture with methanogens at mesophilic temperate (3–11 days) (Wallrabenstein *et al.*, 1995; Harmsen *et al.*, 1998; de Bok *et al.*, 2005; Imachi *et al.*, 2007) and thermophilic temperature (5–9 days) (Imachi *et al.*, 2002; Plugge *et al.*, 2002).

Further quantitative analyses demonstrated presence of MAG 62 (0.3–3.5 log gene copies ng⁻¹ DNA) in various biogas digesters operating at different ammonia levels and propionate levels (0.1–0.9 g NH₃ kg⁻¹ sludge, 0.1–8.0 g propionate L⁻¹) (Table S3), which supports the suggestion that MAG 62 is an ammonia-tolerant bacterium prevalent in biogas systems.

Batch cultivation of the propionate-fed chemostat microbiota was conducted in order to assess the impact of salt and ammonia (5 g L⁻¹ NH₄Cl, 5 g L⁻¹ NaCl or no addition) on propionate degradation and presence of MAG 62. In all batches, the pH varied between 7.3 and 8.0 over the course of the cultivation. In the batches supplemented with NH₄Cl, the ammonia level thus varied between 0.1 and 0.4 g NH₃ L⁻¹. Propionate was completely degraded after 150 days of incubation in all batches. The abundance of MAG 62 were relatively similar in all batches and increased from below detection at day 0 to 1–2 log gene abundance ng⁻¹ DNA after two months of cultivation, indicating that this species tolerates NaCl in addition to NH₄Cl. In line with the results from the biogas digesters, NH₄Cl did not influence the abundance of MAG 62.

Desulfobulbaceae MAG 45

Although MAG 45 represented a minor part of the community in the propionate-fed reactors (0.2% in metagenome sequencing and below detection 16S rRNA gene sequencing), it is still of interest due to its genomic content indicating syntrophic propionate oxidation capability. MAG 45 affiliated with the family Desulfobulbaceae (order Desulfobacteriales, class Deltaproteobacteria) and the closest relative of MAG 45 was *Desulfobulbus propionicus* (73% average nucleotide identity on genome level) (Fig. S4). *D. propionicus* has been demonstrated to achieve growth on propionate and sulphate, but has not been shown to syntrophically degrade propionate with methanogens (Worm *et al.*, 2014). The class Deltaproteobacteria comprises several bacteria capable of syntrophic growth that are also sulphate reducers which oxidise propionate and other organic compounds, with sulphate or fumarate as electron acceptor when available (i.e. the SPOB *Syntrophobacter* and *Syntrophobacterium*) (Morris *et al.*, 2013). Due to its low

relative abundance in the continuously fed reactors, we opted not to give MAG 45 a provisional name.

Methylmalonyl-CoA pathway

MAG 45 can be predicted to encode the capacity for propionate degradation, as it contains an almost complete set of the genes involved in the conventional methylmalonyl-CoA pathway, including the genes *pccAB*, *epi*, *mut* (encoding methylmalonyl-CoA mutase), *sucD*, *frdABC*, *fumABC* and *mdh* (Fig. 4B). In the first step, MAG 45 encodes coenzyme A transferase, previously suggested to be used for activation of propionate in the SPOB *Pelotomaculum schinkii* and *P. propionicum* (Hidalgo-Ahumada *et al.*, 2018). Genes for pyruvate ferredoxin oxidoreductase are absent, but MAG 45 possesses genes encoding 2-oxoacid oxidoreductase (*kor*) that could be used by the bacteria to reduce ferredoxin oxidoreductase and form the energy-rich thioester linkage between CoA and the acyl group.

Metabolic plasticity of MAG 45 is implied by a gene content indicative of sulphate/sulphite-respiring potential (e.g., genes *sat*, *aprAB*, *dsrAB*). Cultivated members of the Desulfobulbaceae are also known to utilise several sulphur compounds as electron acceptors (Pereira *et al.*, 2011), while some species reduce ferric iron (Knoblauch *et al.*, 1999). Members of this family have also been suggested to function as a syntrophic partner with Peptococcaceae during benzene degradation (Kunapuli *et al.*, 2007). However, as sulphate and ferric iron were absent from the enrichments in the present study, it is more likely that MAG 45 persisted in the propionate-fed reactors using syntrophic activity.

H₂/formate production and energy conservation systems

The energy conservation system of MAG 45 indicates that electrons from the membrane-bound succinate dehydrogenase can be transferred to NADH-quinone oxidoreductase units (*nuoC-N*), which couples the oxidation of NADH to the reduction of quinone (Schut *et al.*, 2016). Similarly to MAG 62, MAG 45 encodes F-type ATP synthase and *fixAB* (Table S6). MAG 45 also encodes the trimeric quinone-modifying oxidoreductase complex (*qmoABC*), which can link the electron transfer chain to the first reductive step of sulphate reduction or the final step of sulphite reduction (Hocking *et al.*, 2014). This oxidoreductase complex has also been suggested to transfer electrons between cytoplasmic enzymes and periplasmic formate and hydrogen dehydrogenases in syntrophic propionate degradation by *Syntrophobacterium fumaroxidans* (Sedano-Nunez *et al.*, 2018).

Genes associated with hydrogenases, including [FeFe] group ABC and [NiFe] group 1abcd, 3bc, 4ae (Table S7),

heterodisulphide reductase (*hdr*) and the soluble [NiFe] hydrogenase/heterodisulphide-like (*mvh*), were annotated. These enzymes can form a complex that uses a bifurcating coupling mechanism to reduce heterodisulphide and ferredoxin simultaneously, with H₂ as reductant (Kaster *et al.*, 2011), which is suggested to be indicative of microorganisms specialising in low-energy metabolism (Sedano-Nunez *et al.*, 2018). Genes encoding membrane-bound hydrogenases (*hyaABD*) and their associated homologs required for biosynthesis of [NiFe]-hydrogenases (*hypA-hypF*) (Peters *et al.*, 2015) were annotated. MAG 45 was also found to encode cytochrome bd ubiquinol oxidase units, which are often needed to anchor the hydrogenase complex to the membrane and allow electron transfer to the quinone pool (Peters *et al.*, 2015). Formate dehydrogenase units (including *fdoHI*, *fdhE*, *iscS*) with associated molybdenum co-factors were annotated. Cytochrome c and manganese-dependent pyrophosphatase, which can be involved in energy conservation (Pereira *et al.*, 2011), were also found.

Other metabolic capabilities, membrane transport, sporulation and motility

Genes for a high-affinity phosphate (P_i) transport system (*pst*), including genes for regulatory and Pi-sensing/regulatory proteins (Hudek *et al.*, 2016), were identified. The *pst* gene has previously been found in putative SPOB (Dyksma and Gallert, 2019) and has been shown to be of importance for growth of sulphate-reducing Deltaproteobacteria under phosphate-limited conditions (Bosak *et al.*, 2016). MAG 45 contains genes for glycolysis and the citric acid cycle, while presence of a lactate dehydrogenase complex indicates that MAG 45 has capacity for lactate utilisation. Gene annotations indicate some resistance to oxidative stress, and a majority of genes required for biosynthesis of B₁₂ were found (Table S6).

Genetic potential for ammonia and pH tolerance and the overall genomic potential of the two SPOB candidates

In contrast to other known SPOB (Liu and Lu, 2018), but similarly to ammonia-tolerant syntrophic acetate-oxidising bacteria (Manzoor *et al.*, 2018), MAG 62 and MAG 45 were found to lack genes for assimilation of ammonium (e.g., the ammonium permease encoding gene, *amtB*) or some other ammonium transporter that might impede redundant ammonium influx (Manzoor *et al.*, 2015). Another similarity to known ammonia-tolerant syntrophic acetate-oxidising bacteria is that MAG62 and MAG 45 possess genes for a transporter-complex involved in glycine, betaine and carnitine or

proline uptake (*gbuABC* and *proVWX*, respectively) (Tables S4, S6). The *gbu* and *pro* porters have been shown to be used to accumulate these substances inside the cell, where they function as compatible solutes and protect the cell under high osmotic stress conditions (Mendum and Smith, 2002). Glycine and betaine are examples of quaternary ammonium compounds, but actual involvement of the *gbu/pro* transporter as an osmoprotectant against ammonia stress has yet to be demonstrated. In MAG 62, genes for an enzyme that maintains cytoplasmic pH and sodium tolerance in alkaline environments (*mrpA-G*) (Ito *et al.*, 2017) were also found.

To get an overview of the total genomic potential of MAG 62 and MAG 45, we constructed sequence similarity networks based on approximately 15 000 protein families in the Pfam database of these two candidate SPOB and their closest relatives (*P. propionicicum* and *D. propionicus*, respectively). These networks resulted in protein clusters based on the known functions (Figs. S6, S7). However, a large number of the proteins present in MAG 62 and 45 and the known SPOB could not be clustered (based on the analytical parameters). This is due to the limitations of the databases, where approximately half the proteins are unknown/hypothetical or do not have a known biological function. It is possible that some genes which were missing for our SPOB candidates are structurally different from other known proteins, and therefore could not be annotated. It is thus highly likely that some tasks are carried out by proteins that are yet to be identified and characterised.

Methanogenic populations

The methanogenic community was represented by two MAGs, MAG 28 and MAG 54. MAG 54 belongs to *M. bourgensis* (98% average nucleotide identity) (Fig. S5), which is suggested to be one of the most preferred H₂/formate users in syntrophic acetate oxidation (Westerholm *et al.*, 2016; Westerholm *et al.*, 2018a,b). The genome of this species has been thoroughly described (Manzoor *et al.*, 2016; Maus *et al.*, 2016a). Metagenome sequencing also indicated presence of another *Methanoculleus* sp. (MAG 28) representing 6% of the total metagenome coverage (similar to the *M. bourgensis* MAG 54 coverage) (Fig. S3). Based on whole-genome phylogeny, the most closely related species to MAG 28 was “*Candidatus Methanoculleus thermohydrogenotrophicus*” (sp. DTU006) (Kougias *et al.*, 2017) (Fig. 5). The genomic average nucleotide identity and genome-to-genome distance of MAG 28 to known methanogenic species was < 87% (Fig. S5) and 28%, respectively, and thus below the thresholds for defining new species (Goris *et al.*, 2007;

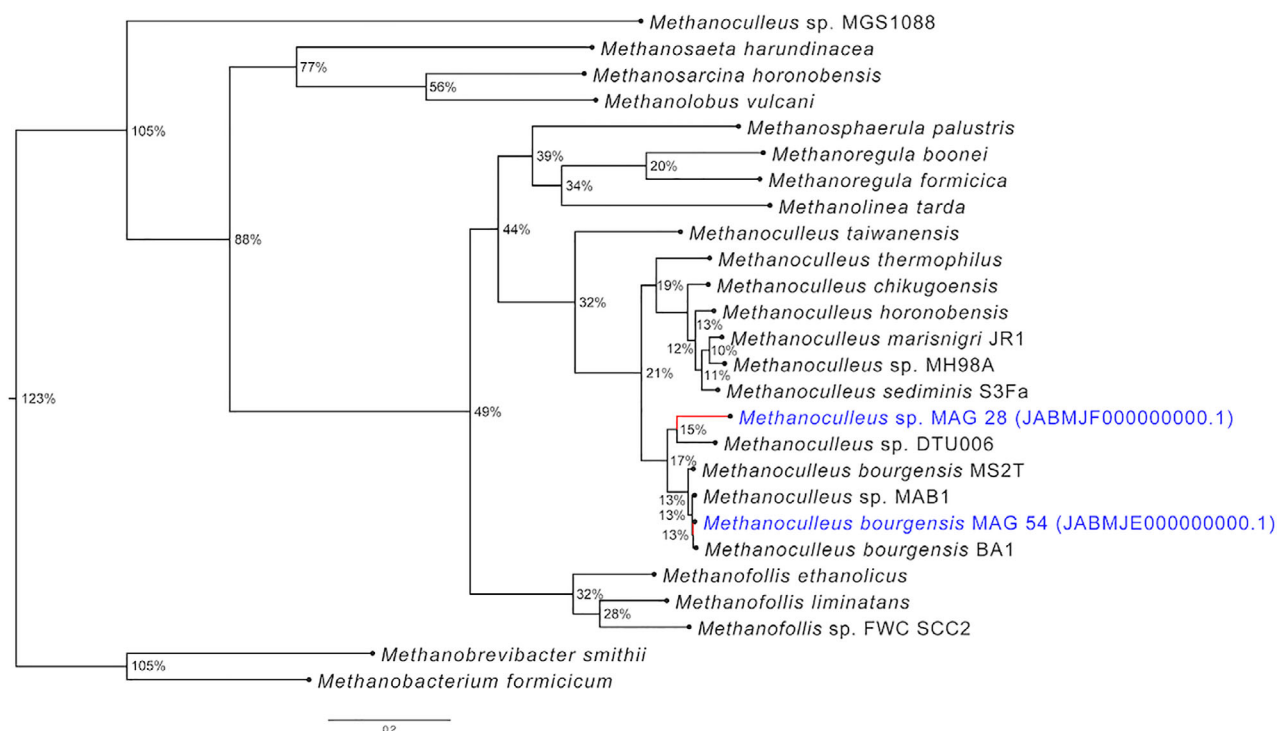


Fig 5. Phylogenetic positioning of *Methanoculleus*-associated metagenome assembled genomes (MAG 28 and MAG 54) retrieved from propionate-fed chemostats in the present study. [Color figure can be viewed at wileyonlinelibrary.com]

Jain *et al.*, 2018). In order to confirm that the species represented by MAG 28 represents a novel methanogenic species, a genome with higher completeness must be recovered in future research. MAG 28 encodes the complete methanogenesis pathway from hydrogen, including genes for various [NiFe]-hydrogenases (*echA-F*, *ehaB-P*, *mvhADG*). MAG 28 also has the majority of the genes for flavin-based electron bifurcation (*hdrABC*, *vhuADUG*, *fwdA-G*, *fdhBD*) (Table S8), in which exergonic heterodisulfide reduction is coupled to and drives the initial endergonic reduction of CO₂ to formylmethanofuran with H₂-derived electrons (Milton *et al.*, 2018). Similarly to *M. bourgensis* MS2^T and MAB1, MAG 28 does not contain genes related to ammonium transport systems, but has genes for a glycine betaine/proline transport system that can facilitate osmotic stress adaptation (Maus *et al.*, 2015; Manzoor *et al.*, 2016).

The reason for the co-existence of the two different *Methanoculleus* species in the propionate-fed reactors is difficult to deduce from the results of the present study. Both methanogens represented by MAG 28 and MAG 54 were also found in a continuously acetate-fed reactor (unpublished data). Future research is needed to reveal the roles of these two methanogens.

Evaluation of possible involvement in propionate conversion by other taxa in the propionate-fed reactors

The 16S rRNA gene sequencing results indicated that bacteria belonging to the families Caldicoprobacteraceae and Ruminococcaceae (Firmicutes), Synergistaceae (genus *Aminobacterium*, phylum Synergistetes) and Porphyromonadaceae (phylum Bacteroidetes) qualified as potential SPOB. However, the MAGs found to be phylogenetically related to Ruminococcaceae, *Aminobacterium* or Porphyromonadaceae lacked a majority of genes in the conventional methylmalonyl-CoA and the dismutation pathway for propionate oxidation (data not shown). Unfortunately, no high-quality MAG taxonomically associated with Caldicoprobacteraceae was retrieved in the present study. Furthermore, when several strains with identical 16S rRNA gene similarity to *Aminobacterium colombiense* were isolated from the different reactors and co-cultivated in medium containing acetate with hydrogenotrophic methanogen or propionate with a syntrophic acetate oxidising co-culture, acid degradation was not initiated in any of these cultures (unpublished data). This indicates that this species was not directly involved in propionate or acetate degradation in the continuously fed reactors in the present study. As

A. colombiense produces acetate as the main product, but also propionate from certain amino acids and carboxyl acids (Baena *et al.*, 1998), it could potentially provide substrate for the prevailing syntrophic bacteria in the reactors through degradation of yeast components in the medium. However, the higher relative abundance of *Aminobacterium* in the propionate-fed than in the acetate-fed reactors is puzzling.

To conclude, in this study we described the genomes of putative ammonia-tolerant syntrophic propionate-oxidising bacteria “*Ca. Syntrophopropionicum ammoniitolerans*” and MAG 45, a novel genus in the families Peptococcaceae and Desulfobulbaceae, respectively. The assembled genomes of these putative SPOB contained an almost complete set of the genes involved in the conventional methylmalonyl-CoA pathway, whereas the majority of genes required for the dismutation pathway were missing. “*Ca. Syntrophopropionicum ammoniitolerans*” was shown to distinctly diverge from SPOB affiliating with *Pelotomaculum*, *Smithella*, *Syntrophobacter*, *Syntrophobacterium* and “*Candidatus Cloacamonas*”, which are known to represent dominant syntrophic propionate degraders in low-ammonia and mesophilic (30–40°C) anaerobic digesters (Ariasyady *et al.*, 2007b; Ban *et al.*, 2015; Ahlert *et al.*, 2016; Wang *et al.*, 2019). Our results also suggest that conversion of propionate to methane at high ammonia was conducted through cooperation between “*Ca. Syntrophopropionicum ammoniitolerans*,” an ammonia-tolerant syntrophic acetate-oxidising bacterium (Clostridiaceae sp.), and the methanogens *Methanoculleus bourgensis* and a novel *Methanoculleus* species.

Experimental Procedures

Anaerobic reactor set-up and operation

Four identical laboratory-scale continuously stirred (80 rpm) tank reactors (Belach Bioteknik, Stockholm, Sweden) with working volume 1.1 L were operated in parallel at 37°C in continuous mode. The reactors were fed continuously with anoxic and sterile bicarbonate-buffered basal medium (BM) (Westerholm *et al.*, 2010) including yeast extract (0.2 g L⁻¹) and trace elements and vitamins (e.g., Zn, Ca, Mn, Mo, Al, Co, Ni, Se, vitamin B₁₂ and biotin). Two reductants to remove traces of oxygen, cysteine-HCl (0.5 g L⁻¹) and NaS (0.24 g L⁻¹), were added to the BM. The BM was supplemented with 16 g NH₄Cl L⁻¹ and 0.1 M sodium propionate (equal to 9.6 g sodium propionate L⁻¹, P1 and P2) or 16 g NH₄Cl L⁻¹ and 0.1 M sodium acetate (equal to 8.9 g sodium acetate L⁻¹, A1 and A2). The initial pH of the BM was 7.3, but increased during operation to around

8.1, where it stayed stable without any further additions throughout the experimental period. The reactors were inoculated with 1 L sterile BM and 0.1 L sludge during flushing with N₂. The inoculum consisted of sludge from a mesophilic high-ammonia (5.4 g NH₄⁺-N L⁻¹, 0.6–0.9 g NH₃ L⁻¹) laboratory-scale digester degrading food waste and albumin, referred to as D^{TE}37 in Westerholm *et al.* (2015). The biogas digester was supplemented with trace elements, which was essential for the biogas process in order to avoid accumulation of short-chain fatty acids. Previous microbial studies on the source digester have demonstrated dominance of syntrophic acetate oxidation as the main pathway for methanisation of acetate (Westerholm *et al.*, 2015; Müller *et al.*, 2016). In the present study, the four continuously-fed reactor compartments were fed with peristaltic pumps (Belach Bioteknik) at a dilution rate of 26 µl min⁻¹ to obtain a hydraulic retention time of 28 days. Short-chain fatty acid concentrations (acetate, propionate, butyrate, isobutyrate, valerate, isovalerate, capronate and isocapronate) were analysed using high performance liquid chromatography (HPLC) and methane content in the gas was determined by gas chromatography (GC) on a weekly basis as described previously (Westerholm *et al.*, 2018b). The gas produced was collected in gas bags and the volume was measured using a gas counter meter. The reactors operated under constant feeding for 144 days (with the exception of P2, which encountered a technical error and had to be shut down after 115 days of operation).

DNA extraction, 16S rRNA gene amplicon sequencing and data analysis

Total microbial community DNA was extracted from samples taken on nine occasions throughout operation (after 17, 31, 45, 66, 88, 94, 101, 109, 115 days of operation). These samples were stored at -20°C until used for analysis. DNA extraction, construction of 16S rRNA gene amplicon libraries using primers 515F (GTGBCAGC MGCCGCGGTAA) (Hugerth *et al.*, 2014) and 805R (GACTACHVGGGTATCTAATCC) (Herlemann *et al.*, 2011), and Illumina sequencing of 16S rRNA gene amplicon libraries were performed as described by Müller *et al.* (2016). Paired-end sequencing was performed on an Illumina MiSeq instrument (Eurofins GATC Biotech GmbH, Germany). Illumina adapters and primer sequences were trimmed using Cutadapt v. 2.2 (Martin, 2017). Generation of amplicon sequence variants (ASV), abundance table and taxonomic assignments of ASVs were determined using the package *dada2* (v. 1.6.0) (Callahan *et al.*, 2016) in R (v. 3.4.0) on the SLUBI computing cluster in Uppsala (running on CentOS Linux release 7.1.1503; module handling by Modules based on Lua: v. 6.0.1; <https://www.slubi.se/>). Taxonomic classification of

the 16S rRNA gene sequence variants was done using the Silva taxonomic training dataset v132 formatted for DADA2 (McLaren, 2020). A phyloseq object was created using abundance and taxonomy tables for visualisation of community structure with the package *phyloseq* (version 1.30.0) (McMurdie and Holmes, 2013) in RStudio version 3.5.2 (RStudio Team, 2015).

Metagenomic sequencing, assembly, binning and functional analysis

Metagenomic sequencing was performed on samples from the parallel propionate-fed reactors withdrawn at day 115 and was conducted using Illumina HiSeq, with 2 × 150 bp pair-end reads (Eurofins Genomics, Germany). Sequence data from the two reactors were filtered for adapter sequences and quality processed using Atropos. The data were then combined and assembled using SPADES (Didion *et al.*, 2017; Nurk *et al.*, 2017). Both datasets were mapped towards the assembled contigs using bowtie2 (Langmead and Salzberg, 2012), and binning was performed using Metabat2 and quality controlled using CheckM (Kang *et al.*, 2015; Parks *et al.*, 2015), resulting in both a placement tree and a table for bin quality. Good-quality bins were selected and further investigated by visualisation of their placement in the tree, using the package *ggtree* in R to focus on specific clades of interest (Yu *et al.*, 2017; R Core Team, 2018). MAGs that were of interest based on their phylogenetic affiliation were annotated using the program Prokka version 1.14 (Seemann, 2014). Annotations for the MAGs were further corrected by the EnrichM pipeline (v. 0.5.0) using the profile HMMs (evalue 1e-05) of KEGG (Kyoto Encyclopedia of Genes and Genomes) protein reference modules (Boyd *et al.*, 2019). Annotated MAGs were manually validated for the genes involved in the methylmalonyl-CoA pathway with the assistance of the KEGG database (Kanehisa *et al.*, 2014). A threshold of 70% genome completeness was established for further phylogenetic analysis. Hydrogenase gene sequences were extracted from the MAGs and manual classification was carried out against the curated hydrogenases database HydDB (accessed 2020-04) (Søndergaard *et al.*, 2016).

Genome-to-genome distances between retrieved MAGs and genomes of closest relatives were determined using the Genome-to-Genome Distance Calculator v. 2.1, which mimics conventional DNA-DNA hybridisation (Meier-Kolthoff *et al.*, 2013). The relative abundance of each MAG was estimated by calculating the proportion of mapped reads to each MAG relative to total amount of reads. Whole-genome percentage average nucleotide identity (ANI) was calculated with the pyani Python module (v. 0.2.10) (Pritchard *et al.*, 2016) with blast+ algorithm,

and visualisation was done in RStudio with the package *ggplot2* (v. 3.2.1) (Wickham, 2016). Sequence similarity networks (SSN) for MAG 45 and MAG 62 were generated with the online tool EFI-EST (accessed 2020-04) (Zallot *et al.*, 2019) using the amino acid sequences with the default parameters. Visualisation and network rendering were done in Cytoscape v. 3.7.2 (Shannon *et al.*, 2003). The species trees for the methanogens and SPOBs were created by the Species Tree inference from All Genes (STAG) method implemented in Orthofinder v.n 2 (Emms and Kelly, 2018; Emms and Kelly, 2019). The 16S rRNA gene sequences from the methanogens were retrieved from the National Centre for Biotechnological Information (NCBI) RefSeq database and aligned using default parameters in MAFFT aligner v. 7.3 (Kato and Standley, 2013). A phylogenetic tree with the aligned 16S rRNA gene sequences was generated with the software Fasttree (v. 2.1.10) (Price *et al.*, 2009) with Jukes-Cantor (JC) distance and maximum likelihood (ML) topology refinement with 10 rounds of nearest-neighbour interchange (NNI) and five rounds of subtree pruning and regrafting (SPR). The generalised time-reversible (GTR) model was run with 10 rounds of CAT approximation and GAMMA rate heterogeneity and BIONJ distance optimisation, together with 1000 bootstrap iterations. Visualisation and annotation of all phylogenetic trees were done in Figtree v. 1.4.3 (Rambaut, 2009).

Available genomes from previously known or predicted SPOB were downloaded from the database at NCBI. Raw sequence data from 16S rRNA gene amplicon sequencing and metagenomics sequencing are available under NCBI BioProject PRJNA625873. The MAG sequences have been deposited at DDBJ/ENA/GenBank under the accession JABMJD000000000 (MAG 62), JABMJC000000000 (MAG 45), JABMJF000000000 (MAG 28) and JABMJE000000000 (MAG 54).

Quantitative PCR (qPCR)

A quantitative PCR (qPCR) approach targeting the 16S rRNA gene of “*Ca. Syntrophopropionicum ammo nitolerans*” (MAG 62) was set up in order to screen for the gene abundance in the enrichment reactors and in different biogas digesters. The primers AMB₂-433F 5'-ATGACGGTACCCAAGGAGG-3' and AMB₂-596R 5'-GTTTCAAAGGCAGGCTGTGG-3' were designed using Geneious v 10.6.2. The primer specificity was evaluated against the GenBank database using Blast (Altschul *et al.*, 1990). Construction of standard curve was conducted as described previously (Westerholm *et al.*, 2011). In short, the AMB₂ primers were used to amplify the partial 16S rRNA gene of MAG 62 from total DNA extracted from P1 day 115. The purity of the PCR product was checked using Sanger sequencing (Macrogen

Inc.). The PCR product was cloned with a TOPO TA cloning kit (Invitrogen). Plasmid DNA was extracted with a plasmid Mini Kit (Qiagen) and the plasmid concentration was measured by Qubit Fluorometric Quantification (Invitrogen). The qPCR was performed in a 20 μl reaction mixture that consisted of 3 μl DNA template, 10 μl of ORA™ SEE qPCR Green ROX Master Mix (HighQu), 1 μl of each primer (10 pmol μl^{-1}), 8% dimethylsulfoxide (DMSO, Thermo Fisher Scientific) and 1 μg μl^{-1} bovine serum albumin (BSA, Thermo Fisher Scientific). The qPCR protocol for quantification was as follows: 7 min at 95°C, 35 cycles of 95°C for 30 s, annealing at 64°C for 1 min and 72°C for 30 s, and finally temperature melt curve analysis. Reactions were carried out in QuantStudio™ 5 (ThermoFisher). Specificity of the primers was evaluated by Sanger sequencing of the PCR products obtained. The detection limit was about 10² genes ml⁻¹. The abundance of MAG 62 was analysed in samples taken from the enrichment reactors and from two laboratory-scale biogas digesters that operated with increased level of free ammonia (from 0.30 to 1.1 g L⁻¹) through addition of an external nitrogen source or by increasing the organic loading rate (OLR from 3.2 to 6.0 g short-chain solids L⁻¹ day). A full description of the reactor operation can be found in a previous publication (Moestedt *et al.*, 2016). The abundance of MAG 62 was also analysed in a laboratory-scale digester (R_{lab}) fed the organic fraction of municipal solid waste. This digester operated at mesophilic temperature conditions and the ammonia level increased as a consequence of gradually increased levels of albumin (Table S3).

Batch cultivation

Batch cultivations were conducted to evaluate growth of MAG 62 in presence of NaCl or NH₄Cl or without extra salt (in addition to the 0.3 g L⁻¹ included in the medium). Inoculum taken from the propionate-fed reactors was inoculated in 250 L serum bottles containing 75 ml BM with 50 mM sodium propionate. The anaerobic bottles were prepared as described elsewhere (Westerholm *et al.*, 2019). Triplicate batches containing 5 g L⁻¹ NH₄Cl, 5 g L⁻¹ NaCl or no salt addition (in addition to 0.3 g NH₄Cl L⁻¹ and 0.3 g NaCl L⁻¹ included in the BM) were prepared. pH was measured regularly during growth and the ammonia level was calculated using the equation given in Westerholm *et al.* (2016). Propionate degradation and methane production in the batches were measured using HPLC and GC, respectively.

Acknowledgements

The authors wish to thank Simon Isaksson for assistance with reactor operation and Christian Brandt for help and guidance

in metagenomic analysis. We are grateful for Oskar Karlsson Lindsjö for contribution to the experimental design and preliminary analysis, and critical review of the paper. This research was supported by the Swedish Research Council for Environment, Agricultural Sciences and Spatial Planning (Formas) under grant number 2012-808, and by the Swedish Energy Agency (2014-000725).

Conflict of Interest

The authors have no conflict of interest to declare.

References

- Ahlert, S., Zimmermann, R., Ebling, J., and König, H. (2016) Analysis of propionate-degrading consortia from agricultural biogas plants. *MicrobiologyOpen* **5**: 1027–1037.
- Ahring, B.K. (2003) Perspectives for anaerobic digestion. In *Advances in Biochemical Engineering/Biotechnology – Biomethanation I*, Ahring, B.K. (ed). Berlin: Springer, pp. 1–30.
- Altschul, S.F., Gish, W., Miller, W., Myers, E.W., and Lipman, D.J. (1990) Basic local alignment search tool. *J Mol Biol* **215**: 403–410.
- Ariesyady, H.D., Ito, T., and Okabe, S. (2007a) Functional bacterial and archaeal community structures of major trophic group in a full-scale anaerobic sludge digester. *Water Res* **41**: 1554–1568.
- Ariesyady, H.D., Ito, T., Yoshiguchi, K., and Okabe, S. (2007b) Phylogenetic and functional diversity of propionate-oxidizing bacteria in an anaerobic digester sludge. *Appl Microbiol Biotechnol* **75**: 673–683.
- Baena, S., Fardeau, M.L., Labat, M., Ollivier, B., Thomas, P., Garcia, J.L., and Patel, B.K.C. (1998) *Aminobacterium colombiense* gen. nov. sp. nov., an amino acid-degrading anaerobe isolated from anaerobic sludge. *Anaerobe* **4**: 241–250.
- Ban, Q., Zhang, L., and Li, J. (2015) Shift of propionate-oxidizing bacteria with HRT decrease in an UASB reactor containing propionate as a sole carbon source. *Appl Biochem Biotechnol* **175**: 274–286.
- Baykov, A.A., Malinen, A.M., Luoto, H.H., and Lahti, R. (2013) Pyrophosphate-fueled Na⁺ and H⁺ transport in prokaryotes. *Microbiol Mol Biol Rev* **77**: 267–276.
- Bertran, E., Ward, L.M., and Johnston, D.T. (2020) Draft genome sequence of *Desulfofundulus thermobenzoicus* subsp. thermosyntrophicus DSM 14055, a moderately thermophilic sulfate reducer. *Microbiol Resour Announce* **9**: e01416–e01419.
- de Bok, F.A.M., Harmsen, H.J.M., Plugge, C.M., de Vries, M. C., Akkermans, A.D.L., De Vos, W.M., and Stams, A.J.M. (2005) The first true obligately syntrophic propionate-oxidizing bacterium, *Pelotomaculum schnikii* sp. nov., co-cultured with *Methanospirillum hungatei*, and emended description of the genus *Pelotomaculum*. *Int J Syst Evol Microbiol* **55**: 1697–1703.
- de Bok, F.A.M., Plugge, C.M., and Stams, A.J.M. (2004) Interspecies electron transfer in methanogenic propionate degrading consortia. *Water Res* **38**: 1368–1375.

- de Bok, F.A.M., Stams, A.J.M., Dijkema, C., and Boone, D. R. (2001) Pathway of propionate oxidation by a syntrophic culture of *Smithella propionica* and *Methanospirillum hungatei*. *Appl Environ Microbiol* **67**: 1800–1804.
- Bonk, F., Popp, D., Weinrich, S., Straeuber, H., Kleinstueber, S., Harms, H., and Centler, F. (2018) Ammonia inhibition of anaerobic volatile fatty acid degrading microbial communities. *Front Microbiol* **9**: 2921.
- Boone, D.R., and Bryant, M.P. (1980) Propionate-degrading bacterium, *Syntrophobacter wolinii* sp. nov. gen. nov., from methanogenic ecosystems. *Appl Environ Microbiol* **40**: 626–632.
- Bosak, T., Schubotz, F., de Santiago-Torio, A., Kuehl, J.V., Carlson, H.K., Watson, N., et al. (2016) System-wide adaptations of *Desulfovibrio alaskensis* G20 to phosphate-limited conditions. *PLoS One*, **11**: e0168719.
- Boyd, J.A., Woodcroft, B.J., and Tyson, G.W. (2019) *Comparative genomics using EnrichM*, 1: <https://github.com/geronimp/enrichM>.
- Buckel, W., and Thauer, R.K. (2018) Flavin-based electron bifurcation, a new mechanism of biological energy coupling. *Chemi Rev* **118**: 3862–3886.
- Callahan, B.J., McMurdie, P.J., Rosen, M.J., Han, A.W., Johnson, J.A., and Holmes, S.P. (2016) DADA2: High-resolution sample inference from Illumina amplicon data. *Nat Methods* **13**: 581–583.
- Capson-Tojo, G., Moscoviz, R., Astals, S., Robles, A., and Steyer, J.P. (2020) Unraveling the literature chaos around free ammonia inhibition in anaerobic digestion. *Renew Sustain Energy Rev* **117**: 109487.
- Chen, J.L., Ortiz, R., and Steele, T.W.J. (2014) Toxicants inhibiting anaerobic digestion: A review. *Biotechnol Adv* **32**: 1523–1534.
- Chen, S., Liu, X., and Dong, X. (2005) *Syntrophobacter sulfatireducens* sp. nov., a novel syntrophic, propionate-oxidizing bacterium isolated from UASB reactors. *Inter J Syst Evol Microbiol* **55**: 1319–1324.
- Chen, Y.T., Zeng, Y., Wang, H.Z., Zheng, D., Kamagata, Y., Narihiro, T., et al. (2020) Different interspecies electron transfer patterns during mesophilic and thermophilic syntrophic propionate degradation in chemostats. *Microb Ecol* **80**: 120–132.
- Cotton, C.A.R., Edlich-Muth, C., and Bar-Even, A. (2018) Reinforcing carbon fixation: CO₂ reduction replacing and supporting carboxylation. *Curr Opin Biotechnol* **49**: 49–56.
- Didion, J.P., Martin, M., and Collins, F.S. (2017) Atropos: specific, sensitive, and speedy trimming of sequencing reads. *PeerJ* **5**: e3720.
- Dolfing, J. (2014) Thermodynamic constraints on syntrophic acetate oxidation. *Appl Environ Microbiol* **80**: 1539–1541.
- Dyksma, S., and Gallert, C. (2019) Candidatus *Syntrophosphaera thermopropionivorans*: a novel player in syntrophic propionate oxidation during anaerobic digestion. *Environ Microbiol Report* **11**: 558–570.
- Eloe-Fadrosch, E.A., Ivanova, N.N., Woyke, T., and Kyrpides, N.C. (2016) Metagenomics uncovers gaps in amplicon-based detection of microbial diversity. *Nat Microbiol*, **1**, 1.
- Emms, D.M., and Kelly, S. (2018) STAG: Species tree inference from all genes. *BioRxiv - The Preprint Server for Biology*, 1: 1–29. <https://doi.org/10.1101/267914>.
- Emms, D.M., and Kelly, S. (2019) OrthoFinder: phylogenetic orthology inference for comparative genomics. *Genome Biol* **20**: 238.
- Galushko, A., & Kuever, J. (2021). *Syntrophobacterium* gen. nov.. M.E. Trujillo S. Dedysch P. DeVos B. Hedlund P. Kämpfer F.A. Rainey & W.B. Whitman *Bergey's Manual of Systematics of Archaea and Bacteria*.
- Goris, J., Konstantinidis, K.T., Klappenbach, J.A., Coenye, T., Vandamme, P., and Tiedje, J.M. (2007) DNA-DNA hybridization values and their relationship to whole-genome sequence similarities. *IJSEM* **57**: 81–91.
- Green, L.K., La Flamme, A.C., and Ackerley, D.F. (2014) *Pseudomonas aeruginosa* MdaB and WrbA are water-soluble two-electron quinone oxidoreductases with the potential to defend against oxidative stress. *J Microbiol* **52**: 771–777.
- Hao, L.P., Michaelsen, T.Y., Singleton, C.M., Dottorini, G., Kirkegaard, R.H., Albertsen, M., et al. (2020) Novel syntrophic bacteria in full-scale anaerobic digesters revealed by genome-centric metatranscriptomics. *ISME J* **14**: 906–918.
- Harmsen, H.J.M., van Kuijk, B.L.M., Plugge, C.M., Akkermans, A.D.L., De Vos W.M., & Stams, A.J.M. (1998) *Syntrophobacter fumaroxidans* sp. nov., a syntrophic propionate-degrading sulfate reducing bacterium. *Int J Syst Bacteriol* **48**: 1383–1387.
- Herlemann, D.P.R., Labrenz, M., Jürgens, K., Bertilsson, S., Waniek, J.J., and Andersson, A.F. (2011) Transitions in bacterial communities along the 2000km salinity gradient of the Baltic Sea. *ISME J* **5**: 1571–1579.
- Hidalgo-Ahumada, C.A.P., Nobu, M.K., Narihiro, T., Tamaki, H., Liu, W.-T., Kamagata, Y., et al. (2018) Novel energy conservation strategies and behaviour of *Pelotomaculum schinkii* driving syntrophic propionate catabolism. *Environ Microbiol* **20**: 4503–4511.
- Hocking, W.P., Stokke, R., Roalkvam, I., and Steen, I.H. (2014) Identification of key components in the energy metabolism of the hyperthermophilic sulfate-reducing archaeon *Archaeoglobus fulgidus* by transcriptome analyses. *Front Microbiol* **5**: 95.
- Hudek, L., Premachandra, D., Webster, W.A.J., and Brau, L. (2016) Role of phosphate transport system component PstB1 in phosphate internalization by *Nostoc punctiforme*. *Appl Environ Microbiol* **82**: 6344–6356.
- Hugerth, L.W., Wefer, H.A., Lundin, S., Jakobsson, H.E., Lindberg, M., Rodin, S., et al. (2014) DegePrime, a program for degenerate primer design for broad-taxonomic range PCR in microbial ecology studies. *Appl Environ Microbiol* **80**: 5116–5123.
- Imachi, H., Sakai, S., Ohashi, A., Harada, H., Hanada, S., Kamagata, Y., and Sekiguchi, Y. (2007) *Pelotomaculum propionicicum* sp. nov., an anaerobic, mesophilic, obligately syntrophic, propionate-oxidizing bacterium. *Int J Syst Evol Microbiol* **57**: 1487–1492.
- Imachi, H., Sekiguchi, Y., Kamagata, Y., Hanada, S., Ohashi, A., and Harada, H. (2002) *Pelotomaculum thermopropionicum* gen. nov., sp. nov., an anaerobic, thermophilic, syntrophic propionate-oxidizing bacterium. *Int J Syst Evol Microbiol* **52**: 1729–1735.
- Ishii, S., Kosaka, T., Hori, K., Hotta, Y., and Watanabe, K. (2005) Coaggregation facilitates interspecies hydrogen transfer between *Pelotomaculum thermopropionicum* and

- Methanothermobacter thermautotrophicus*. *Appl Environ Microbiol* **71**: 7838–7845.
- Ito, M., Morino, M., and Krulwich, T.A. (2017) Mrp antiporters have important roles in diverse bacteria and archaea. *Front Microbiol* **8**: 2325.
- Jain, C., Rodriguez-R, L.M., Phillippy, A.M., Konstantinidis, K.T., and Aluru, S. (2018) High throughput ANI analysis of 90K prokaryotic genomes reveals clear species boundaries. *Nature Commun* **9**: 5114.
- James, K.L., Rios-Hernandez, L.A., Wofford, N.Q., Mouttaki, H., Sieber, J.R., Sheik, C.S., et al. (2016) Pyrophosphate-dependent ATP formation from acetyl coenzyme A in *Syntrophus aciditrophicus*, a new twist on ATP formation. *Mbio* **7**: e01208–e01216.
- Kanehisa M, Goto S, Sato Y, Kawashima M, Furumichi M, Tanabe M (2014). Data, information, knowledge and principle: back to metabolism in KEGG. *Nucleic Acids Research*, **42**, (D1), D199–D205. <http://dx.doi.org/10.1093/nar/gkt1076>.
- Kang, D.W.D., Froula, J., Egan, R., and Wang, Z. (2015) MetaBAT, an efficient tool for accurately reconstructing single genomes from complex microbial communities. *PeerJ* **3**: e1165.
- Kaster, A.-K., Moll, J., Parey, K., and Thauer, R.K. (2011) Coupling of ferredoxin and heterodisulfide reduction via electron bifurcation in hydrogenotrophic methanogenic archaea. *Proceed Nat Acad Sci* **108**: 2981–2986.
- Kato, S., Kosaka, T., and Watanabe, K. (2009) Substrate-dependent transcriptomic shifts in *Pelotomaculum thermopropionicum* grown in syntrophic co-culture with *Methanothermobacter thermautotrophicus*. *Microb Biotechnol* **2**: 575–584.
- Katoh, K., and Standley, D.M. (2013) MAFFT Multiple Sequence Alignment Software Version 7: Improvements in Performance and Usability. *Mol Biol Evol* **30**: 772–780.
- Kirkegaard, R.H., Mclroy, S.J., Kristensen, J.M., Nierychlo, M., Karst, S.M., Dueholm, M.S., et al. (2017) The impact of immigration on microbial community composition in full-scale anaerobic digesters. *Sci Report* **7**: 9343.
- Knoblauch, C., Sahm, K., and Jorgensen, B.B. (1999) Psychrophilic sulfate-reducing bacteria isolated from permanently cold Arctic marine sediments: description of *Desulfotrigulus oceanense* gen. nov., sp nov., *Desulfotrigulus fragile* sp nov., *Desulfofaba gelida* gen. nov., sp nov., *Desulfotalea psychrophila* gen. nov., sp nov and *Desulfotalea arctica* sp nov. *IJSEM* **49**: 1631–1643.
- Kosaka, T., Kato, S., Shimoyama, T., Ishii, S., Abe, T., and Watanabe, K. (2008) The genome of *Pelotomaculum thermopropionicum* reveals niche-associated evolution in anaerobic microbiota. *Genome Res* **18**: 442–448.
- Kougias, P.G., Campanaro, S., Treu, L., Zhu, X., and Angelidaki, I. (2017) A novel archaeal species belonging to *Methanoculleus* genus identified via de-novo assembly and metagenomic binning process in biogas reactors. *Anaerobe* **46**: 23–32.
- Kunapuli, U., Lueders, T., and Meckenstock, R.U. (2007) The use of stable isotope probing to identify key iron-reducing microorganisms involved in anaerobic benzene degradation. *ISME J* **1**: 643–653.
- Langmead, B., and Salzberg, S.L. (2012) Fast gapped-read alignment with Bowtie 2. *Nat Method* **9**: 357–U354.
- Li, Y., Sun, Y., Li, L., and Yuan, Z. (2018) Acclimation of acid-tolerant methanogenic propionate-utilizing culture and microbial community dissecting. *Bioresour Technol* **250**: 117–123.
- Liu, P., and Lu, Y. (2018) Concerted metabolic shifts give new insight into the syntrophic mechanism between propionate-fermenting *Pelotomaculum thermopropionicum* and hydrogenotrophic *Methanocella conradii*. *Front Microbiol* **9**: 1551.
- Liu, Y., Balkwill, D.L., Aldrich, H.C., Drake, G.R., and Boone, D.R. (1999) Characterization of the anaerobic propionate-degrading syntrophs *Smithella propionica* gen. nov., sp. nov. and *Syntrophobacter wolinii*. *Inter J Syst Bacteriol* **49**: 545–556.
- Manzoor, S., Bongcam-Rudloff, E., Schnürer, A., and Müller, B. (2015) Genome-guided analysis and whole transcriptome profiling of the mesophilic syntrophic acetate oxidising bacterium *Syntrophaceticus schinkii*. *PLoS One* **11**: e0166520.
- Manzoor, S., Schnürer, A., Bongcam-Rudloff, E., and Müller, B. (2016) Complete genome sequence of *Methanoculleus bourgensis* strain MAB1, the syntrophic partner of mesophilic acetate-oxidising bacteria (SAOB). *Stand Genom Sci*, **11**: 80.
- Manzoor, S., Schnürer, A., Bongcam-Rudloff, E., and Müller, B. (2018) Genome-guided analysis of *Clostridium ultunense* and comparative genomics reveal different strategies for acetate oxidation and energy conservation in syntrophic acetate-oxidising bacteria. *Genes* **9**: 225.
- Martin, M. (2017) Cutadapt removes adapter sequences from high-throughput sequencing reads. <https://doi.org/10.14806/ej.17.1.200>.
- Maus, I., Koeck, D.E., Cibis, K.G., Hahnke, S., Kim, Y.S., Langer, T., et al. (2016b) Unraveling the microbiome of a thermophilic biogas plant by metagenome and meta-transcriptome analysis complemented by characterization of bacterial and archaeal isolates. *Biotechnol Biofuels* **9**: 171.
- Maus, I., Wibberg, D., Stantscheff, R., Stolze, Y., Blom, J., Eikmeyer, F., et al. (2015) Insights into the annotated genome sequence of *Methanoculleus bourgensis* MS2^T, related to dominant methanogens in biogas-producing plants. *J Biotechnol* **201**: 43–53.
- Maus, I., Wibberg, D., Winkler, A., Puhler, A., Schnurer, A., and Schluter, A. (2016a) Complete genome sequence of the methanogen *Methanoculleus bourgensis* BA1 isolated from a biogas reactor. *Genome Announce* **4**: e00568–e00516.
- McInerney, M.J., Sieber, J.R., and Gunsalus, R.P. (2009) Syntrophy in anaerobic global carbon cycles. *Curr Opin Biotechnol* **20**: 623–632.
- McLaren, M.R. (2020) Silva SSU Taxonomic Training Data Formatted for DADA2. In. <https://zenodo.org/>. <https://doi.org/10.5281/zenodo.3731176>.
- McMurdie, P.J., and Holmes, S. (2013) phyloseq: An R package for reproducible interactive analysis and graphics of microbiome census data. *PLoS One* **8**: e61217.
- Meier-Kolthoff, J.P., Auch, A.F., Klenk, H.-P., and Goeker, M. (2013) Genome sequence-based species delimitation with confidence intervals and improved distance functions. *BMC Bioinformatics*, **14**: 60.

- Mendum, M.L., and Smith, L.T. (2002) Gbu glycine betaine porter and carnitine uptake in osmotically stressed *Listeria monocytogenes* cells. *Appl Environ Microbiol* **68**: 5647–5655.
- Milton, R.D., Ruth, J.C., Deutzmann, J.S., and Spormann, A. M. (2018) *Methanococcus maripaludis* employs three functional heterodisulfide reductase complexes for flavin-based electron bifurcation using hydrogen and formate. *Biochemistry* **57**: 4848–4857.
- Moestedt, J., Müller, B., Westerholm, M., and Schnürer, A. (2016) Ammonia threshold for inhibition of anaerobic digestion of thin stillage and the importance of organic loading rate. *Microbial Biotechnol* **9**: 180–194.
- Morales, S.E., and Holben, W.E. (2009) Empirical testing of 16S rRNA gene PCR primer pairs reveals variance in target specificity and efficacy not suggested by in silico analysis. *Appl Environ Microbiol* **75**: 2677–2683.
- Morris, B.E.L., Henneberger, R., Huber, H., and Moissl-Eichinger, C. (2013) Microbial syntrophy: interaction for the common good. *FEMS Microbiol Rev* **37**: 384–406.
- Müller, B., Sun, L., Westerholm, M., and Schnürer, A. (2016) Bacterial community composition and fhs profiles of low- and high-ammonia biogas digesters reveal novel syntrophic acetate-oxidising bacteria. *Biotechnol Biofuel* **9**: 1–18.
- Nakamura, S., and Minamino, T. (2019) Flagella-driven motility of bacteria. *Biomolecules* **9**: 279.
- Nurk, S., Meleshko, D., Korobeynikov, A., and Pevzner, P.A. (2017) metaSPAdes: a new versatile metagenomic assembler. *Genome Res* **27**: 824–834.
- Parks, D.H., Imelfort, M., Skennerton, C.T., Hugenholtz, P., and Tyson, G.W. (2015) CheckM: assessing the quality of microbial genomes recovered from isolates, single cells, and metagenomes. *Genome Res* **25**: 1043–1055.
- Pelletier, E., Kreimeyer, A., Bocs, S., Rouy, Z., Gyapay, G., Chouari, R., et al. (2008) "*Candidatus* Cloacamonas Acidaminovorans": Genome sequence reconstruction provides a first glimpse of a new bacterial division. *J Bacteriol* **190**: 2572–2579.
- Pereira, I.A.C., Ramos, A.R., Grein, F., Marques, M.C., da Silva, S.M., and Venceslau, S.S. (2011) A comparative genomic analysis of energy metabolism in sulfate reducing bacteria and archaea. *Front Microbiol* **2**: 69.
- Peters, J.W., Schut, G.J., Boyd, E.S., Mulder, D.W., Shepard, E.M., Broderick, J.B., et al. (2015) FeFe- and NiFe-hydrogenase diversity, mechanism, and maturation. *Biochim Et Biophys Acta-Mol Cell Res* **1853**: 1350–1369.
- Plugge, C.M., Balk, M., and Stams, A.J.M. (2002) *Desulfotomaculum thermobenzoicum* subsp. *thermosyntrophicum* subsp. nov., a thermophilic, syntrophic, propionate-oxidizing, spore-forming bacterium. *Int J Syst Evol Microbiol* **52**: 391–399.
- Price, M.N., Dehal, P.S., and Arkin, A.P. (2009) FastTree: computing large minimum evolution trees with profiles instead of a distance matrix. *Mol Biol Evol* **26**: 1641–1650.
- Pritchard, L., Glover, R.H., Humphris, S., Elphinstone, J.G., and Toth, I.K. (2016) Genomics and taxonomy in diagnostics for food security: soft-rotting enterobacterial plant pathogens. *Analytic Method* **8**: 12–24.
- R Core Team. (2018) *R: A language and environment for statistical computing*. Vienna, Austria: R Foundation for Statistical Computing.
- Rambaut, A. (2009) A graphical viewer of phylogenetic trees. In *Institute of Evolutionary Biology, Department of Molecular Evolution, Phylogenetics and Epidemiology*, Edinburgh: The university of Edinburgh. <http://tree.bio.ed.ac.uk/software/figtree/>.
- RStudio Team. (2015) *RStudio: integrated development for R*. Boston, MA: RStudio, Inc. <http://www.rstudio.com/>.
- Schink, B. (1997) Energetics of syntrophic cooperation in methanogenic degradation. *Microbiol Molecular Biol Rev* **61**: 262–280.
- Schut, G.J., Zadovnyy, O., Wu, C.H., Peters, J.W., Boyd, E. S., and Adams, M.W.W. (2016) The role of geochemistry and energetics in the evolution of modern respiratory complexes from a proton-reducing ancestor. *Biochim Biophys Acta Bioenergetics* **1857**: 958–970.
- Sedano-Nunez, V.T., Boeren, S., Stams, A.J.M., and Plugge, C.M. (2018) Comparative proteome analysis of propionate degradation by Syntrophobacter fumaroxidans in pure culture and in coculture with methanogens. *Environment Microbiol* **20**: 1842–1856.
- Seemann, T. (2014) Prokka: rapid prokaryotic genome annotation. *Bioinformatics* **30**: 2068–2069.
- Shannon, P., Markiel, A., Ozier, O., Baliga, N.S., Wang, J.T., Ramage, D., et al. (2003) Cytoscape: A software environment for integrated models of biomolecular interaction networks. *Genome Res* **13**: 2498–2504.
- Shigematsu, T., Era, S., Mizuno, Y., Ninomiya, K., Kamegawa, Y., Morimura, S., and Kida, K. (2006) Microbial community of a mesophilic propionate-degrading methanogenic consortium in chemostat cultivation analyzed based on 16S rRNA and acetate kinase genes. *Appl Microbiol Biotechnol* **72**: 401–415.
- Sieber, J.R., McInerney, M.J., and Gunsalus, R.P. (2012) Genomic insights into syntrophy: the paradigm for anaerobic metabolic cooperation. *Ann Rev Microbiol* **66**: 429–452.
- Søndergaard, D., Pedersen, C.N.S., and Greening, C. (2016) HydDB: A web tool for hydrogenase classification and analysis. *Sci Rep* **6**: 34212.
- Stams, A.J.M., and Plugge, C.M. (2009) Electron transfer in syntrophic communities of anaerobic bacteria and archaea. *Nature Reviews* **7**: 568–577.
- Vanwonterghem, I., Jensen, P., Dennis, P.G., Hugenholtz, P., Rabaey, K., and Tyson, G.W. (2014) Deterministic processes guide long-term synchronised population dynamics in replicate anaerobic digesters. *ISME J* **8**: 2015–2028.
- Wallrabenstein, C., Hauschild, E., and Schink, B. (1995) *Syntrophobacter pfennigii* sp. nov., new syntrophically propionate-oxidizing anaerobe growing in pure culture with propionate and sulfate. *Arch Microbiol* **164**: 346–352.
- Wang, H.-Z., Lv, X.-M., Yi, Y., Zheng, D., Gou, M., Nie, Y., et al. (2019) Using DNA-based stable isotope probing to reveal novel propionate- and acetate-oxidizing bacteria in propionate-fed mesophilic anaerobic chemostats. *Sci Report* **9**: 17396–17396.
- Westerholm, M., Dolfig, J., and Schnürer, A. (2019) Growth characteristics and thermodynamics of syntrophic acetate oxidizers. *Environ Sci Technol* **53**: 5512–5520.
- Westerholm, M., Dolfig, J., Sherry, A., Gray, N.D., Head, I. M., and Schnürer, A. (2011) Quantification of syntrophic

- acetate-oxidizing microbial communities in biogas processes. *Environ Microbiol Reports* **3**: 500–505.
- Westerholm, M., Isaksson, S., Karlsson Lindsjö, O., and Schnürer, A. (2018a) Microbial community adaptability to altered temperature conditions determines the potential for process optimisation in biogas production. *Appl Energy* **226**: 838–848.
- Westerholm, M., Moestedt, J., and Schnürer, A. (2016) Biogas production through syntrophic acetate oxidation and deliberate operating strategies for improved digester performance. *Appl Energy* **179**: 124–135.
- Westerholm, M., Müller, B., Isaksson, S., and Schnürer, A. (2015) Trace element and temperature effects on microbial communities and links to biogas digester performance at high ammonia levels. *Biotechnol Biofuel* **8**: 1–19.
- Westerholm, M., Müller, B., Singh, A., Karlsson Lindsjö, O., and Schnürer, A. (2018b) Detection of novel syntrophic acetate-oxidising bacteria from biogas processes by continuous acetate enrichment approaches. *Microbial Biotechnol* **11**: 680–693.
- Westerholm, M., Roos, S., and Schnürer, A. (2010) *Syntrophaceticus schinkii* gen. nov., sp. nov., an anaerobic, syntrophic acetate-oxidizing bacterium isolated from a mesophilic anaerobic filter. *FEMS Microbiol Lett* **309**: 100–104.
- Wickham, H. (2016). *ggplot2: Elegant graphics for data analysis*, 2(1–260). New York: Springer.
- Worm, P., Koehorst, J.J., Visser, M., Sedano-Núñez, V.T., Schaap, P.J., Plugge, C.M., et al. (2014) A genomic view on syntrophic versus non-syntrophic lifestyle in anaerobic acid degrading communities. *Biochim Biophys Acta* **1837**: 2004–2016.
- Yu, G.C., Smith, D.K., Zhu, H.C., Guan, Y., and Lam, T.T.Y. (2017) GGtree: an R package for visualization and annotation of phylogenetic trees with their covariates and other associated data. *Method Ecol Evol* **8**: 28–36.
- Zalot, R., Oberg, N., and Gerlt, J.A. (2019) The EFI web resource for genomic enzymology tools: Leveraging protein, genome, and metagenome databases to discover novel enzymes and metabolic pathways. *Biochemistry* **58**: 4169–4182.
- Zheng, D., Wang, H., Gou, M., Nubo, M.K., Narihiro, T., Hu, B., et al. (2019) Identification of novel potential acetate-oxidizing bacteria in thermophilic methanogenic chemostats by DNA stable isotope probing. *Appl Microbiol Biotechnol* **103**: 8631–8645.

Supporting Information

Additional Supporting Information may be found in the online version of this article at the publisher's web-site:

Appendix S1: Supporting information.

Table S4: Gene annotations in MAG 62.

Table S5: Hydrogenase gene annotations in MAG 62.

Table S6: Gene annotations in MAG 45.

Table S7: Hydrogenase gene annotations in MAG 45.

Table S8: Gene annotations in MAG 28.